Scientia Iranica, Vol. 11, No. 4, pp 332–338

SCIENTIA IRANICA

Vapor Absorption into Liquid Films Flowing over a Column of Cooled Horizontal Tubes

B. Farhanieh* **and F. Babadi**[1]

In this paper, a theoretical analysis of the combined heat and mass transfer over cooled horizontal tubes is presented. The boundary layer assumptions are used for the transport of mass, momentum and energy equations and the finite difference method is employed to solve the governing equations in the absorber tube bundle. The effects of important parameters, such as solution flow rate, absorber pressure and tube radius, are discussed on the overall heat and mass transfer for a tube and tube bundle.

INTRODUCTION

Absorption of vapor into liquid films is encountered in many applications. One of the processes most considered is that which occurs in the absorber of absorption chillers. In the absorber, the water vapor produced by the evaporator is absorbed by a concentrated lithium bromide solution flowing over cooled horizontal tubes. The absorption of vapor at the interface of the liquid film is an exothermic process, therefore, the coolant water flowing into the tubes removes the excess heat from the film.

The combined heat and mass transfer process over horizontal tubes does not lend itself easily to mathematical analysis. Most of the published literature deals with modeling the absorption process in a laminar film flowing down an inclined plane.

The first model that attempted to solve a complete formulation of this problem was published by Grigoreva and Nakoryakov [1]. A series solution was used to solve governing partial differential equations. Subsequently, a similar solution to the previous problem was used in a second paper [2]. Grossman carried out theoretical analysis to calculate the absorption of gases in both laminar and turbulent liquid film [3,4]. He considered, also, the effect of non-absorbable gases on the combined heat and mass transfer process [5]. A detailed theoretical model was developed for the film, taking into consideration bulk movements in the vapor and liquid phases in the direction perpendicular to the molar flux due to concentration gradients in the absorbent and vapor.

Andberg and Vliet presented a simplified model for absorption of vapor into liquid films flowing over cooled horizontal tubes with the aid of boundary layer assumptions for transport of mass, momentum and energy [6]. Choudhary developed a finite difference method based on boundary layer assumptions and the method of contour lines and profiles for various conditions and studied the effect of some parameters on the heat and mass transfer process [7].

Several experimental studies have been performed for absorption of water vapor into an aqueous lithium bromide solution. Cosenza and Vliet presented the heat transfer coefficient in terms of a film Nusselt number as a function of a film Reynolds number [8]. Deng and Ma reported the results of experimental studies on the characteristics of a falling film absorber made up of 24 rows of horizontal smooth tubes [9]. The results show that while the mass transfer coefficient is increased as the spray density increases, the heat transfer coefficient is increased only in small spray density ranges. Kyung and Herold studied the effect of absorber inlet sub-cooling, solution flow rate, mass fraction and concentration of additives on the heat transfer coefficient [10].

In this paper, the heat and mass transfer phenomena, which occur on the tube bundle of an absorber, is modeled using boundary layer assumptions. The finite difference method is employed for solving the governing equations.

PROBLEM FORMULATION

The problem to be studied is presented schematically in Figure 1. The solution entering the absorber flows

*. *Corresponding Author, Department of Mechanical Engineering, Sharif University of Technology, Tehran, I.R. Iran.*

1. *Department of Mechanical Engineering, Sharif University of Technology, Tehran, I.R. Iran.*

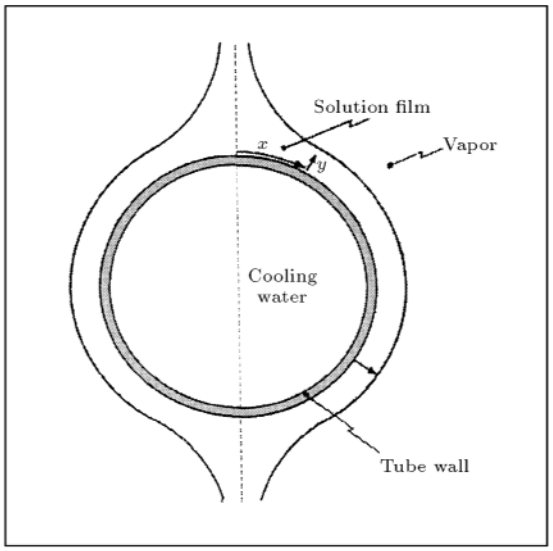

Figure 1. The schematic diagram of a film flowing over a cooled horizontal tube.

down over horizontal tubes. The mass transfer process occurs at the interface of the flowing film and the vapor coming from the evaporator. The vapor is absorbed by the strong concentrated film and the heat produced due to this process is rejected by external cooling water which flows inside the tubes.

The flow is studied under the following assumptions:

a. The equilibrium condition exists at the film interface between the film and the vapor at the absorber pressure;

b. There is no shear force between the liquid film and the vapor;

c. The flow is laminar and there are no waves at the film interface;

d. The film thickness variation, due to the substance absorbed into the solution, is negligible;

e. The heat transfer to the vapor phase is negligible;

f. The inertia and pressure gradient effects are negligible and the flow is buoyancy driven;

g. The turning jet effect at the top section of the tube is negligible compared to the viscous region on the tube.

The momentum equation and the boundary conditions for the falling film are:

$$\mu\frac{\partial^2 u}{\partial y^2} = \rho g \sin\theta, \tag{1}$$

$$\text{At } y = 0, \qquad u = 0, \tag{2}$$

$$\text{At } y = \delta, \qquad \frac{\partial u}{\partial y} = 0, \tag{3}$$

where $\theta = \frac{x}{r}$. The momentum equation is solved for x-component of the velocity:

$$u = \frac{\rho g}{\mu}\sin\left(\frac{x}{r}\right)\left[\delta y \quad \frac{1}{2}y^2\right]. \tag{4}$$

The y-component of the velocity field is determined from the continuity equation:

$$v = \frac{\rho g y^2}{2\mu}\left[\frac{d\delta}{dx}\sin\left(\frac{x}{r}\right) + \frac{1}{r}\left(\delta \quad \frac{y}{3}\right)\cos\left(\frac{x}{r}\right)\right]. \tag{5}$$

The mass flow rate of the film is evaluated by:

$$m = \int_0^{\delta} \rho u(y) dy. \tag{6}$$

The film thickness can now be determined by:

$$\delta = \left[\frac{3\mu m}{\rho^2 g \sin\left(\frac{x}{r}\right)}\right]^{\frac{1}{3}}. \tag{7}$$

Neglecting the viscous dissipation term and considering the above mentioned assumptions, the energy and species transport equations read as:

$$u\frac{\partial T}{\partial x} + v\frac{\partial T}{\partial y} = \alpha\frac{\partial^2 T}{\partial y^2}, \tag{8}$$

$$u\frac{\partial \omega}{\partial x} + v\frac{\partial \omega}{\partial y} = D\frac{\partial^2 \omega}{\partial y^2}. \tag{9}$$

To obtain the distribution of temperature and concentration fields and, hence, the heat and mass transfer coefficients, the above equations are solved numerically using the following boundary and initial conditions:

$$\text{At } x = x_i \quad \text{and} \quad 0 < y < \delta:$$

$$T = T_i \quad \text{and} \quad \omega = \omega_i, \tag{10}$$

$$\text{At} \quad x_i < x \quad \text{and} \quad y = 0:$$

$$T = T_w \quad \text{and} \quad \frac{\partial \omega}{\partial y} = 0. \tag{11}$$

The film surface temperature is determined by the equilibrium condition in its concentration and absorber pressure:

$$\text{At} \quad x_i < x \quad \text{and} \quad y = \delta:$$

$$T = T_s(\omega_s, P) \quad \text{and} \quad \omega = \omega_s. \tag{12}$$

Indicating that the surface concentration and the temperature are related by the equilibrium condition. From Fick's law of diffusion:

$$\text{At} \quad x_i < x \quad \text{and} \quad y = \delta: \quad m'' = \frac{\rho D}{\omega_s}\frac{\partial \omega}{\partial y}. \tag{13}$$

The heat produced by the absorption process is:

$$q = m'' L, \tag{14}$$

and is diffused through the film towards the tube surface:

$$\text{At} \quad x_i < x \quad \text{and} \quad y = \delta : \quad q = \quad k\frac{\partial T}{\partial y}. \tag{15}$$

SOLUTION METHODOLOGY

In order to extend the capabilities of the finite difference method to deal with complex geometries, a boundary fitted coordinate is used.

The basic idea in this method is to map the complex flow domain in the physical space to a simple rectangular domain in the computational space by using a curvilinear coordinate transformation:

$$\varepsilon = \frac{x}{\pi r}, \tag{16}$$

$$\eta = \frac{y}{\delta(x)}, \tag{17}$$

where r is the tube outer radius. In other words, the Cartesian coordinate system in the physical domain is replaced by a general non-orthogonal system. The obtained transformed governing equations are:

$$u = \left(\frac{\rho g \delta^2 \sin(\pi\varepsilon)}{\mu}\right)\left(\eta \quad \frac{1}{2}\eta^2\right), \tag{18}$$

$$v = \quad \frac{\rho g \delta^2 \eta^2}{2\mu r}\left[\frac{1}{\pi}\frac{d\delta}{d\varepsilon}\sin'(\pi\varepsilon) + \delta\left(1 \quad \frac{\eta}{3}\right)\cos(\pi\varepsilon)\right], \tag{19}$$

$$\frac{\partial T}{\partial \varepsilon} = \left(\frac{\pi r \alpha}{u\delta^2}\right)\frac{\partial^2 T}{\partial \eta^2} + \left[\frac{\eta}{\delta}\frac{d\delta}{d\varepsilon} \quad \frac{\pi r v}{\delta u}\right]\frac{\partial T}{\partial \eta}, \tag{20}$$

$$\frac{\partial \omega}{\partial \varepsilon} = \left(\frac{\pi r D}{u\delta^2}\right)\frac{\partial^2 \omega}{\partial \eta^2} + \left[\frac{\eta}{\delta}\frac{d\delta}{d\varepsilon} \quad \frac{\pi r v}{\delta u}\right]\frac{\partial \omega}{\partial \eta}. \tag{21}$$

The variation of boundary layer thickness is determined using Equation 7:

$$\frac{d\delta}{d\varepsilon} = \quad \left(\frac{\mu m \pi^3}{9\rho^2 g}\right)^{\frac{1}{3}} \frac{1}{\sin^{\frac{1}{3}}(\pi\varepsilon)\,.\,\tan(\pi\varepsilon)}. \tag{22}$$

The transformed form of the initial and boundary conditions and of the equilibrium equations becomes:

$$\text{At} \quad \varepsilon = \varepsilon_i \quad \text{and} \quad 0 < \eta < 1 :$$

$$T = T_i \quad \text{and} \quad \omega = \omega_i, \tag{23}$$

$$\text{At} \quad \varepsilon_i < \varepsilon \quad \text{and} \quad \eta = 0 :$$

$$T = T_w \quad \text{and} \quad \frac{\partial \omega}{\partial \eta} = 0, \tag{24}$$

$$\text{At} \quad \varepsilon_i < \varepsilon \quad \text{and} \quad \eta = 1 :$$

$$T = T_s(\omega_s, P) \quad \text{and} \quad \omega = \omega_s, \tag{25}$$

$$m'' = \frac{\rho D}{\delta}\frac{1}{\omega_s}\frac{\partial \omega}{\partial \eta}, \tag{26}$$

$$q = m'' L = \quad \frac{k}{\delta}\frac{\partial T}{\partial \eta}. \tag{27}$$

The equations are discretised by using a fully implicit method in the flow direction and an iterative procedure is used at each step to find temperature and concentration profiles.

COMPUTATIONAL DETAILS

The numerical domain is divided into N nodes in the flow and M nodes across the transversal directions.

It is evident from Figure 1 that the boundary layer thickness at the inlet and outlet region of the flow around the tube is infinity and could not be calculated in a regular manner. Thus, the numerical calculation starts from the third point ($I = 3$) and ends at point $I = N \quad 2$.

SOLUTION ALGORITHM

The sequence of the solution algorithm can be stated as:

1. Calculate the velocity field and boundary layer thickness at each step by Equations 18 and 19;
2. Guess the absorbed mass flux at the film surface at each step;
3. Solve Equation 21 to obtain the concentration profile;
4. Determine the surface concentration;
5. By assuming that the surface is at equilibrium with the vapor at the absorber pressure, use Equation 25 to obtain the surface equilibrium temperature;
6. Solve Equation 20 for the temperature profile in the cross section of the film;
7. Solve Equation 27 for the mass flux of the absorbed vapor;
8. Check for the convergence criteria set for the mass flux;
9. If the criteria is not satisfied, return to step 1. Otherwise, the convergence in the solution is achieved.

GRID SIZE EFFECTS

In order to investigate grid size effects, runs were performed with $20\times40, 40\times80, 80\times160, 120\times240, 160\times$

320, 200 × 400 and 240 × 480 grid points, respectively. The flow-wise velocity profiles for these grids are plotted in Figure 2. A 120 × 240 mesh was chosen in the final calculations to maintain reasonable accuracy.

RESULTS

The case studies are carried out for real conditions. The fluid properties are taken from [11]. The effect of important parameters, such as mass flow rate, absorber pressure and tube radius on the heat transfer coefficient, was determined.

The inlet temperature and concentration for lithium bromide flow are taken as 51°C and 64%, respectively. The absorber pressure is considered to be 800 Pa, which is the pressure during real operating conditions, of a steam fired single effect absorption chiller.

The concentration and temperature distribution through the film are presented in Figures 3 and 4, respectively. The concentration varies through the film flow as the water is absorbed by the concentrated film.

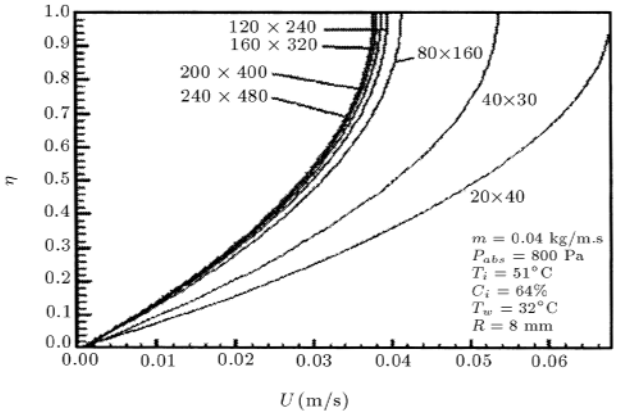

Figure 2. Stream-wise velocity profile U (m/s), at the minimum film thickness for different mesh sizes.

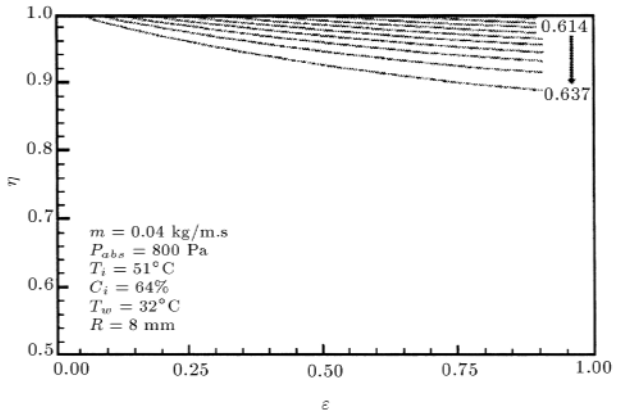

Figure 3. Concentration contours through the flow field for top tube.

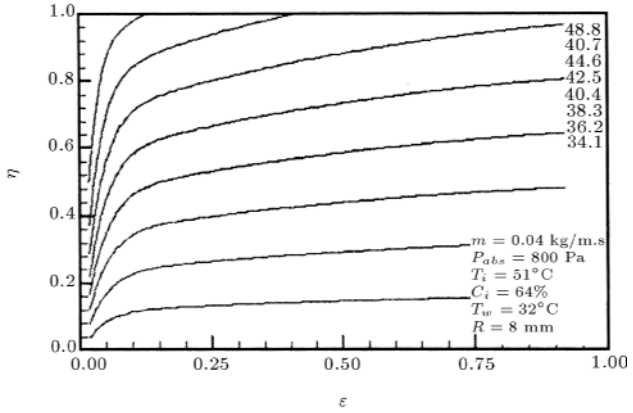

Figure 4. Temperature (°C) contours through the flow field for top tube.

The temperature of the film is reduced through the flow, due to the cooling water stream in the tubes.

Variation of the absorbed mass flux by the concentrated solution is plotted in Figure 5. As can be seen from this figure, due to the high concentration of inlet solution, the absorption rate increases sharply. As the surface concentration of the film reduces, the rate of the absorbed mass flux, after a gentle increase, reduces also. The same pattern is expected for heat transfer through the surface, due to the absorption process.

Since the heat transfer coefficient plays a significant role in the modeling of an absorber, the influences of important parameters on the heat transfer coefficient are investigated and presented.

The average heat transfer coefficient is defined as:

$$\overline{h} = \frac{\overline{q}}{\Delta T_{Ln}}, \tag{28}$$

where ΔT_{Ln} is the log mean temperature difference and is defined as:

$$\Delta T_{Ln} = \frac{(T_i \quad T_w) \quad (T_s \quad T_w)}{Ln\left(\frac{T_i \quad T_w}{T_s \quad T_w}\right)}, \tag{29}$$

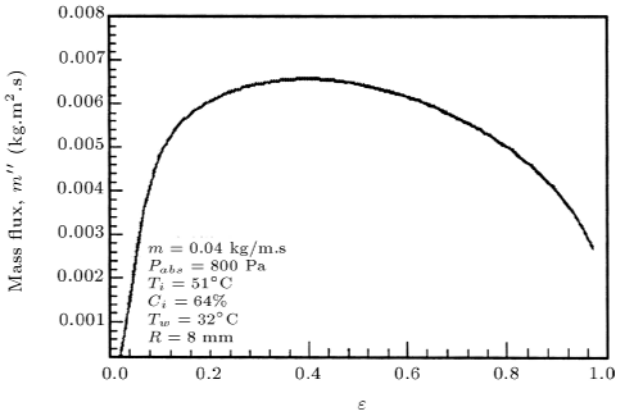

Figure 5. Absorbed mass flux over the top tube (kg/m^{2}s).

T_i and T_s are inlet and surface temperatures of the film flow and T_w is the tube wall temperature.

The effect of solution mass flow rate on the heat transfer coefficient and absorbed mass flux are presented in Figures 6 and 7. Significant decrease in the heat transfer coefficient is observed as the mass flow rate increases, due to the increase in boundary layer thickness. It can be seen that the absorbed mass flux decreases by increasing the mass flow rate.

The increase in the absorber pressure increases the heat transfer coefficient slightly (see Figure 8). The effect of tube radius on the heat transfer coefficient is investigated and presented in Figure 9. The heat transfer coefficient decreases linearly by increasing the tube radius. However, at small radii (less than one inch), the heat transfer coefficient is constant and has its highest value.

Unfortunately there is not a lot of experimental data in the literature that permits true verification of the current model for a wide range of parameters. Even though data from a well-defined experiment is not available, it is possible to test the model against the overall change in solution temperature or concentration for an entire absorber tube column. The results of experimental data for twelve test conditions are tabulated in [6] and are compared to current numerical results for the outlet solution temperature in Figure 10. The overall agreement of the data with the model is quite good, with an average error of 2%. This implies

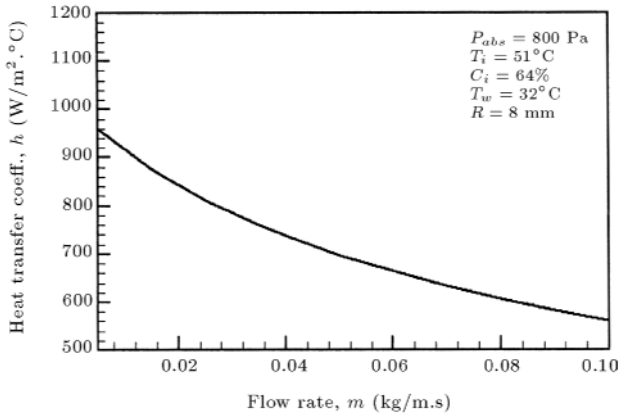

Figure 6. Effect of film flow rate on heat transfer coefficient for top tube.

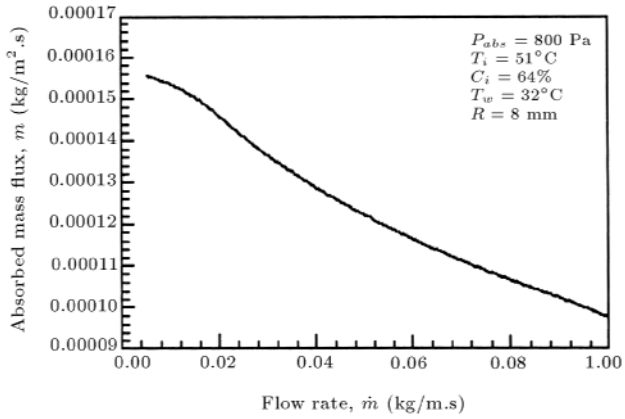

Figure 7. Effect of film flow rate on absorbed mass flux for top tube.

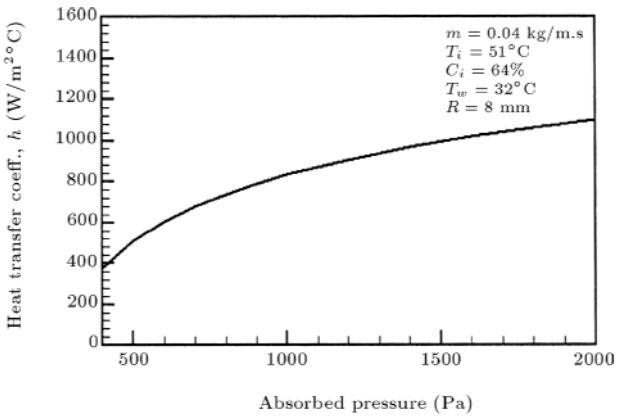

Figure 8. Effect of absorber pressure on heat transfer coefficient.

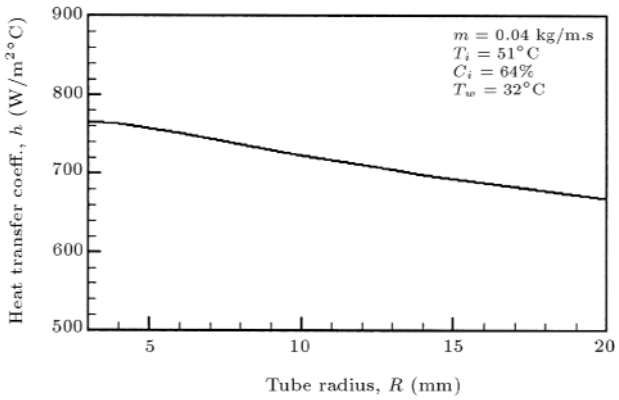

Figure 9. Effect of tube radius on heat transfer coefficient.

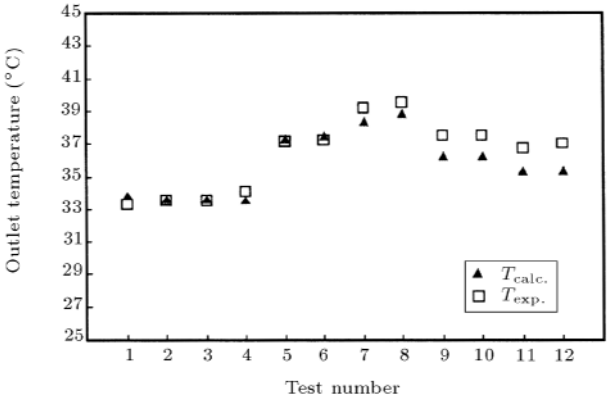

Figure 10. Experimental verification of numerical model for outlet solution temperature for 12 test conditions [6].

that the model describes the physics of the absorption process very well and that the model may be used to analyze an actual absorber tube bundle with acceptable accuracy.

Determining the number of columns and rows in the tube bundle is an important feature in the design process of an absorber.

To extend the results from one tube to a tube bundle or a column of tubes, the mass transfer within the inter-tube space is neglected and the solution inlet conditions for temperature and concentration of a tube are calculated from the outlet conditions of the upper tube. Also, the absorber tube bundle is assumed to be a one-pass coolant-stream; therefore, the tube surface temperature is the same for all tubes in the column.

There are two important factors, which should be taken into account for specifying the number of rows and columns in the tube bundle of an absorber:

1. The amount of vapor produced by the evaporator, which is related to the cooling capacity of the machine;
2. The fluid flow over each tube has a direct influence on the heat and mass transfer of the lower tubes. It is evident from the obtained results that the bulk concentration of the fluid cascading over the lower tubes is reduced (see Figures 11 and 12). Thus, the reduction in concentration reduces the vapor absorption potential of fluid flowing over the lower tubes. Therefore, the effective heat and mass transfer coefficients for tube columns are different from those of single tubes.

The heat and mass transfer for each tube in the tube bundle is presented in Figure 13. It should be noted that increasing the number of tubes in a column increases the construction cost of the tube bundle.

Therefore, there should be a trade-off between maximum mass absorption, total cost and required cooling capacity, for determining the ratio of tube bundle rows and columns (see Figure 14).

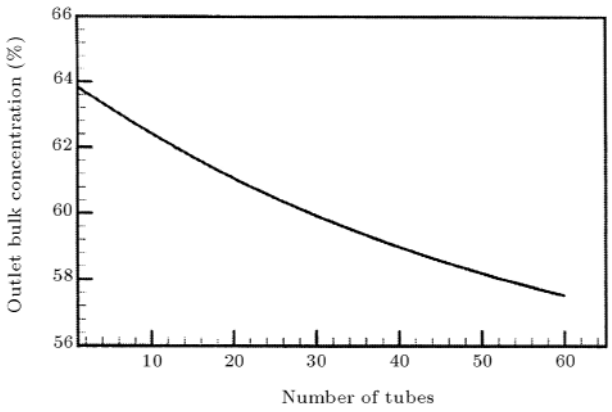

Figure 11. Outlet bulk concentration for various tubes.

CONCLUSIONS

The heat and mass transfer in vapor absorption by laminar liquid film flowing over cooled horizontal tubes is investigated. The velocity field is calculated using the Nusselt theory and the simultaneous energy and diffusion equation are solved to determine the temperature and concentration profiles in the flow field. The

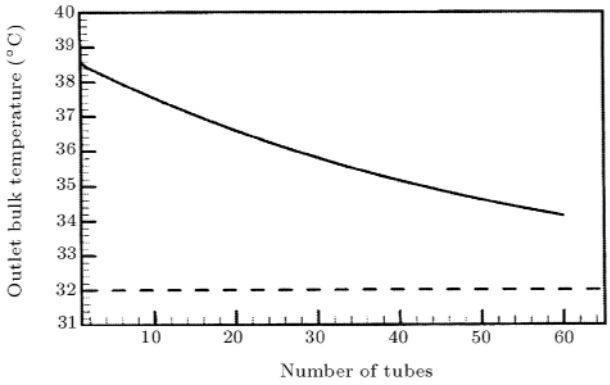

Figure 12. Outlet bulk temperature for various number of tubes.

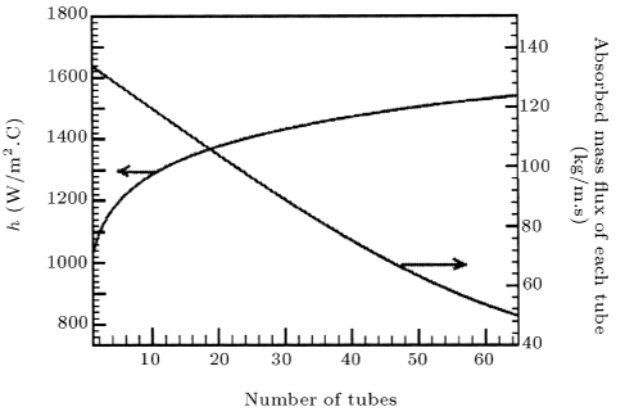

Figure 13. Heat and mass transfer for each tube in the tube bundle.

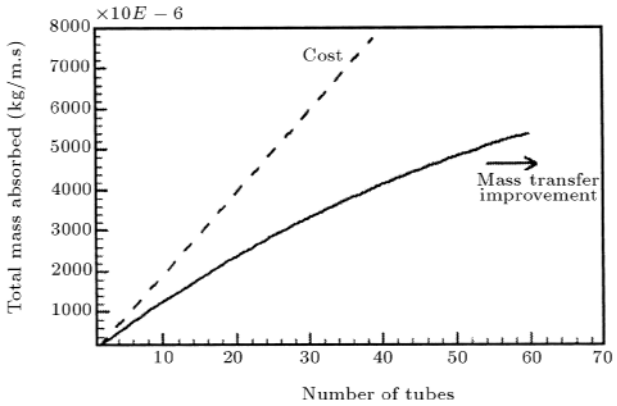

Figure 14. Trade-off between mass transfer improvement and total cost.

effect of important parameters, such as solution flow rate, absorber pressure and tube radius on the overall heat transfer coefficient and total absorbed mass of vapor, is studied. It is shown that determination of the optimum number of rows and columns in an absorber tube bundle needs an accurate trade-off between various important factors, such as cooling capacity, mass transfer improvement and the total capital cost of the absorber.

Also, the current model describes the physics of the absorption process very well and shows that it may be used to analyze an actual absorber tube bundle with acceptable accuracy. The fact that the model predicts the performance of an actual machine quite well suggests that the effect of additives present in commercial units is to improve performance mainly by improving the wetting characteristics of tubes and not by direct action on the absorption process.

NOMENCLATURE

x	axis to flow direction (m)
y	axis perpendicular to flow direction (m)
u	velocity in x direction (m/s)
v	velocity in y direction (m/s)
g	gravitational acceleration (m/s^2)
T	temperature (°C)
P	absorber pressure (Pa)
m	film flow rate (kg/m.s)
m''	absorbed mass flux (kg/m^{2}s)
q	heat flux (W/m^2)
k	thermal conductivity (W/m.K)
D	mass diffusivity (m^2/s)
L	heat of absorption (J/kg)
r	tube radius (m)
M	number of nodes in ε' direction
N	number of nodes in μ direction
ε	non-dimensional x axis
η	non-dimensional y axis
ω	salt (LiBr) mass concentration in the solution
δ	film thickness (m)
θ	angle (radian), equals to $\frac{x}{r}$ or $\pi\varepsilon$
ρ	solution density (kg/m^3)
μ	solution viscosity (kg/m.s)
α	thermal diffusivity (m^2/s)

Subscripts

i	inlet
w	wall
s	surface
Ln	logarithm mean value

REFERENCES

1. Nakoryakov, V.E. and Grigoreva, N.I. "Combined heat and mass transfer during absorption in drops and films", *J. of Engrg. Physics*, **32**(3), pp 243-247 (1977).
2. Grigoreva, N.I. and Nakoryakov, V.E. "Exact solution of combined heat and mass transfer problem during film absorption", *J. of Engrg. Physics*, **33**(5), pp 1349-1353 (1977).
3. Grossman, G. "Simultaneous heat and mass transfer in film absorption under laminar flow", *Int. J. of Heat and Mass Transfer*, **26**(3), pp 357-371 (1983).
4. Grossman, G. and Heat, M.T. "Simultaneous heat and mass transfer in absorption of gases in turbulent liquid films", *Int. J. of Heat and Mass Transfer*, **27**(12), pp 2365-2376 (1984).
5. Grossman, G. and Gommed, K. "Heat and mass transfer in film absorption in the presence of non-absorbable gases", *Int. J. of Heat and Mass Transfer*, **40**(15), pp 3595-3606 (1997).
6. Andberg, J.W. and Vliet, G.C. "A simplified model for absorption of vapors into liquid films flowing over cooled horizontal tubes", *ASHRAE Trans.*, **93**(2), pp 2454-2466 (1987).
7. Choudhary, S.K. et al. "Absorption of vapors into liquid film flowing over cooled horizontal tubes", *ASHRAE Trans.*, **99**(2), pp 81-89 (1993).
8. Cosenza, F. and Vliet, G.C. "Absorption in falling Water/LiBr films on horizontal tubes", *ASHRAE Trans.*, **96**(1), pp 693-701 (1990).
9. Deng, S.M. and Ma, W.B. "Experimental studies on the characteristics of an absorber using LiBr/H_2O solution as working fluid", *Int. J. of Refrigeration*, **22**, pp 293-301 (1999).
10. Kyung, I.S. and Herold, K.E. "Experimental investigation of absorber performance with and without 2-ethyl-hexanol in H_2O-LiBr absorption cycle", *Proceedings of 34th National Heat Transfer Conference*, Pittsburgh, Pennsylvania, USA, pp 322-340 (2000).
11. McNeely, L.A. "Thermodynamic properties of aqueous solutions of lithium bromide", *ASHRAE Trans.*, **85**, pp 413-434 (1979).